Complex and Chaotic Oscillations in a Model for the Catalytic Hydrogen Peroxide Decomposition under Open Reactor Conditions

Guy Schmitz*

Faculté des Sciences Appliqués, Université Libre de Bruxelles, CP165/63, Av. Roosevelt 50, 1050 Bruxelles, Belgium

Ljiljana Kolar-Anić and Slobodan Anić

Faculty for Physical Chemistry, University of Belgrade, P.O. Box 137, Studenski trg 12-16, YU-11001 Beograd, Serbia and Montenegro

Tomislav Grozdić

Center for Multidisciplinary Studies, University of Belgrade, 29 Novembra 142, YU-11000 Beograd, Serbia and Montenegro

Vladana Vukojević

Department of Clinical Neuroscience, Karolinska Institutet, CMM L8:01, 17176 Stockholm, Sweden

Received: June 7, 2006; In Final Form: July 5, 2006

Numerous periodic and aperiodic dynamic states obtained in a model for hydrogen peroxide decomposition in the presence of iodate and hydrogen ions (the Bray−Liebhafsky reaction) realized in an open reactor (CSTR), where the flow rate was the control parameter, have been investigated numerically. Between two Hopf bifurcation points, different simple and complex oscillations and different routes to chaos were observed. In the region of the mixed-mode evolution of the system, the transitions between two successive mixed-mode simple states are realized by period-doubling of the initial state leading to a chaotic window in which the next dynamic state emerges mixed with the initial one. It appears in increasing proportions in concatenated patterns until total domination. Thus, with increasing flow rate the period-doubling route to chaos was obtained, whereas with decreasing flow rate the peak-adding route to chaos was obtained. Moreover, in very narrow regions of flow rates, chaotic mixtures of mixed-mode patterns were observed. This evolution of patterns repeats until the end of the mixed-mode region at high flow rates that corresponds to chaotic mixtures of one large and many small amplitude oscillations. Starting from the reverse Hopf bifurcation point and decreasing the flow rate, simple small amplitude sinusoidal oscillations were encountered and then the period-doubling route to chaos. With a further decreasing flow rate, the mixed-mode oscillations emerge inside the chaotic window.

Introduction

Modeling complex dynamic structures and investigating modes of transition between them is a significant task with a general application to all nonlinear processes irrespective of their nature. Therefore, even though the focus of this study is on the dynamics of one particular example, the Bray−Liebhafsky (BL) reaction, the results obtained are of general relevance for other dynamic systems showing similar complex dynamics.

In the reaction of hydrogen peroxide decomposition in the presence of hydrogen and iodate ions (D), known as the Bray−Liebhafsky reaction,

$$2H_2O_2 \xrightarrow{IO_3^-, H^+} 2H_2O + O_2 \qquad (D)$$
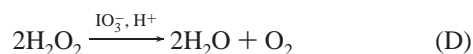
hydrogen peroxide decomposition is the result of two complex pathways in which hydrogen peroxide acts as either a reducing (R) or an oxidizing (O) agent:

$$2IO_3^- + 2H^+ + 5H_2O_2 \rightarrow I_2 + 5O_2 + 6H_2O \qquad (R)$$

$$I_2 + 5H_2O_2 \rightarrow 2IO_3^- + 2H^+ + 4H_2O \qquad (O)$$
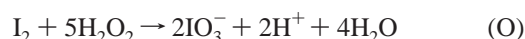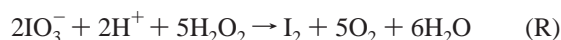
The sum of reactions (R) and (O) gives reaction (D). When the rates of these two pathways are equal, monotonic decomposition of hydrogen peroxide is observed. Studying the kinetics of this system, Bray discovered already in 1921[1] a narrow concentration range where the rates of pathways (R) and (O) are not equal. Under these conditions, pathways (R) and (O) dominate alternately over one another resulting in a cascading consumption of hydrogen peroxide and an oscillatory evolution of the intermediates. The oscillatory dynamics of the BL reaction has been studied extensively in batch reactors.[1−23] However, the complex oscillations, bursts and chaos, obtained in this system when the reaction is realized in a continuously fed well stirred tank reactor (CSTR), have been published only recently.[24,25]

TABLE 1: Model of the Bray−Liebhafsky Reaction

reactions	rate constants[a]	no.
$IO_3^- + I^- + 2 H^+ \rightleftharpoons HIO + HIO_2$	$k_1 = 3.18 \times 10^5$ $k_{-1} = 7.91 \times 10^7$	R1, R-1
$HIO_2 + I^- + H^+ \rightarrow I_2O + H_2O$	$k_2 = 5.0 \times 10^{11}$	R2
$I_2O + H_2O \rightleftharpoons 2HIO$	$k_3 = 5.0 \times 10^3$ $k_{-3} = 3.15 \times 10^8$	R3, R-3
$HIO + I^- + H^+ \rightleftharpoons I_2 + H_2O$	$k_4 = 3.0 \times 10^{11}$ $k_{-4} = 4.5$	R4, R-4
$HIO + H_2O_2 \rightarrow I^- + H^+ + O_2 + H_2O$	$k_5 = 1.20 \times 10^4 +$ $3.0 \times 10^4 [H^+]$	R5
$I_2O + H_2O_2 \rightarrow HIO + HIO_2$	$k_6 = 5.0 \times 10^5$	R6
$HIO_2 + H_2O_2 \rightarrow IO_3^- + H^+ + H_2O$	$k_7 = 2.0 \times 10^3$	R7
$IO_3^- + H^+ + H_2O_2 \rightarrow HIO_2 + O_2 + H_2O$	$k_8 = 9.5 \times 10^{-4} +$ $3.92 \times 10^{-2} [H^+]$	R8

[a] We keep the units mol $\times$ dm^{-3} and min used in the previous papers.[27,32]

The aim of this study is to determine whether the model that was proposed by us[11,26,27] and optimized on the basis of results obtained in a batch reactor can simulate the complex dynamics of the BL reaction in an open reactor. Preliminary results were encouraging.[28]

Model of the Bray−Liebhafsky Reaction

Already in 1921, Bray foundthat the reactions (R) and (O) had to be complex and that the evolution of gaseous oxygen from the system is not the source of oscillatory behavior of the hydrogen peroxide decomposition. Evolution of gaseous oxygen may alter the oscillations, but it is not crucial for their appearing.[29] He also concluded that the oscillatory evolution originates from the complex chemistry between the hydrogen peroxide and intermediate iodine species that appears in the reaction system such as I^-, HIO, and HIO_2. Following his ideas, a model of the mechanism of the overall process was proposed by one of us[11] and later augmented by one[26] and two reactions.[27] All three variants of the model are successful in the simulations of many phenomena in closed and open reactors[26,27,30−35] because the feedback loop is already included in the first model consisting of only six reactions. However, more details of the experimentally observed reaction dynamics can be explained by the version having eight reactions. Our intention in this paper is to see whether complex and chaotic oscillations found experimentally in a CSTR could be simulated by the model given in Table 1 consisting of the eight reactions (R1−R8), where three of them are reversible, with the set of rate constants optimized for batch conditions.[27,32]

In our previous studies,[32] stoichiometric network analysis[36] was used to identify the reactions (R1−R8) that contribute to pathways (R) and (O), calculate the concentrations of the intermediates in the pseudo-steady states and analyze the stability of the steady states. The concentrations of iodate and hydrogen ions are significantly larger than the concentrations of other reactive species and can be considered as constants without qualitatively affecting the results. (Extending the model with two additional differential equations to account for the temporal evolution of these two species does not alter the dynamic structure of the system but only shifts the bifurcation points a little with respect to the flow rate.[28]) Two external species controlling the oscillations are H_2O_2 and I_2. Essential internal species are I^-, HIO, HIO_2, and I_2O. Hence, the temporal evolution of the system is described by the following six differential equations.

$$d[H_2O_2]/dt = -r_5 - r_6 - r_7 - r_8 + j_0([H_2O_2]_{in} - [H_2O_2])$$

$$d[I_2]/dt = r_4 - j_0[I_2]$$

$$d[I^-]/dt = -r_1 - r_2 - r_4 + r_5 - j_0[I^-]$$

$$d[HIO]/dt = r_1 + 2r_3 - r_4 - r_5 + r_6 - j_0[HIO]$$

$$d[HIO_2]/dt = r_1 - r_2 + r_6 - r_7 + r_8 - j_0[HIO_2]$$

$$d[I_2O]/dt = r_2 - r_3 - r_6 - j_0[I_2O]$$

where $[H_2O_2]_{in}$ is the hydrogen peroxide concentration in the input flow, j_0 the specific flow rate (total volume flow divided by the reactor volume), and

$$r_1 = k_1[IO_3^-][I^-][H^+]^2 - k_{-1}[HIO][HIO_2]$$

$$r_2 = k_2[HIO_2][I^-][H^+]$$

$$r_3 = k_3[I_2O] - k_{-3}[HIO]^2$$

$$r_4 = k_4[HIO][I^-] - k_{-4}[I_2]/[H^+]$$

$$r_5 = k_5[HIO][H_2O_2]$$

$$r_6 = k_6[I_2O][H_2O_2]$$

$$r_7 = k_7[HIO_2][H_2O_2]$$

$$r_8 = k_8[IO_3^-][H_2O_2]$$

Numerical Calculations

Calculations were performed using the MATLAB program package. The differential equations derived from the model were integrated using the ode15s solver. The same results were obtained using other numerical integration algorithms available in MATLAB but required longer integration times. Relative and absolute error tolerance values lower than 1×10^{-10} and 1×10^{-18}, respectively, did not influence the results of numerical integrations. Hence, smaller values, in this particular case 3×10^{-14} and 1×10^{-20}, were adopted for the respective error tolerances. The Jacobian was calculated externally. Internal calculation gave the same results but occasionally required longer calculation times.

To discriminate between distinct dynamic patterns and to characterize them accurately, we have used different representations: time sequences, phase space portraits, Poincaré sections, return maps and power spectra. Poincaré sections were also efficient in verifying that the transients had died out and all the presented results describe permanent dynamic states. Power spectra were calculated using the fast Fourier transform routine in MATLAB "fft" function or directly with the "psd" function using Welch's method. The clearer spectra were usually obtained with the "psd" function and a Hamming window (see MATLAB toolkit help file and www.mathworks.com).

Numerical Results

To establish if complex and chaotic oscillations may be reproduced by the model (R1−R8) extended to account for the flow of the species in an isothermal CSTR, numerous numerical simulations using j_0 as the control parameter were performed. The iodate and acid concentrations were maintained constant and equal to the values used in our former simulations,[28] $[IO_3^-] = 0.0474$ and $[H^+] = 0.0958$ mol/dm^3, and the hydrogen

Catalytic H$_2$O$_2$ Decomposition

J. Phys. Chem. A, Vol. 110, No. 34, 2006 **10363**

TABLE 2: Summary of the Numerical Results

j_0 range or value (10^{-3} min^{-1})	pattern[a]	M[b]	k_M[c]	comments
<0.299				stable steady state
0.300−4.8236	1^0			simple large amplitude oscillations
4.8237−4.82455	$(1^0)_2$			period 2, Figure 1
4.82456−4.82476	$(1^0)_{2^p}$	0		sequence of period-doubling
4.82480−4.82592	chaos			Figure 2
4.82593−4.826	**6^1**	0.167	2.69	smallest observed M value
4.8270−4.8291	**4^1**	0.250	3.79	
4.82915−4.82923	$(4^1)_{2^p}$			sequence of period-doubling
4.82925−4.8296	chaos			
4.8297−4.8301	$4^1\,3^1$	0.286	3.75	Figure 3a
4.831	$4^1\,(3^1)_3$	0.308	3.78	
4.8312−4.8316	chaos			
4.8317−4.8360	**3^1**	0.333	3.97	
4.8361−4.8364	$(3^1)_{2^p}$			sequence of period-doubling
4.8366−4.837	chaos			
4.838−4.8421	$3^1\,(2^1)_n$			sequence of peak-adding
4.8422−4.8495	**2^1**	0.500	3.95	
4.8497−4.8502	$(2^1)_{2^p}$			sequence of period-doubling
4.8503	chaos			pattern $(2^1)_n$ without periodicity
4.8504	chaos			mixture of 2^1 and 1^1
4.8505−4.852	$(2^1)_n\,1^1$			
4.855	$2^1\,1^1$	0.667	3.63	
4.860−4.8691	$2^1\,(1^1)_n$			sequence of peak-adding, Figure 3b
4.8692−4.8823	**1^1**	1.00	3.94	longest step in devil's staircase, Figure 5a,b
4.8825−4.88315	$(1^1)_{2^p}$	1.00		sequence of period-doubling, Figure 5c,d
4.8832−4.8848	chaos			Figure 5e,f
4.8849−4.886	$(1^1)_3\,1^2$	1.250	3.66	
4.890−4.906				complicated periodic mixtures of 1^1 and 1^2
4.907	chaos			mixture of $1^1(1^2)_4$ and $1^1(1^2)_5$
4.908−4.9110	$1^1\,(1^2)_n$			sequence of peak-adding
4.9111−4.9195	**1^2**	2.00	3.85	
4.9196−4.92012	$(1^2)_{2^p}$			sequence of period-doubling
4.92015−4.9202	chaos			pattern $(1^2)_n$ without periodicity
4.9210−4.9225	chaos			mixture of 1^2 and 1^3
4.923−4.924	$(1^2)_2\,1^3$	2.333	3.79	
4.925	chaos			mixture of 1^2 and 1^3
4.926	$1^2(1^21^3)_3$	2.429	3.78	
4.930	$1^2\,1^3$	2.500	3.68	
4.933−4.939	$1^2\,(1^3)_n$			sequence of peak-adding
4.940−4.945	**1^3**	3.00	3.85	
4.946−4.9463	$(1^3)_{2^p}$			sequence of period-doubling
4.9464−4.9466	chaos			
4.947	$(1^3)_3\,1^4$	3.250	3.80	
4.950−4.960				complicated periodic mixtures of 1^3 and 1^4
4.961−4.965	**1^4**	4.00	3.88	
4.966−4.96608	$(1^4)_{2^p}$			sequence of period-doubling
4.967	chaos			mixture of 1^4 and 1^5
4.968	$(1^4)_2\,1^5$	4.333	3.83	
4.977−4.981	**1^5**	5.00	3.91	
4.990	**1^6**	6.00	3.93	Figure 3c
5.004−5.0810	1^n			n increases from 7 to 35 with narrow chaotic windows
5.0812−5.0816				chaos and crisis at about 5.0815, Figure 4
5.0817−5.082	$(0^1)_{2^p}$ [d]			sequence of period-halving
5.085−5.1196	0^1			small limit cycle
>5.120				stable steady state

^{a} l^s represents a sequence of l consecutive large amplitude oscillations followed by s consecutive small ones. ^{b} Ratio between the total number S of small amplitude oscillations and the total number L of large ones. The firing numbers are equal to $M/(1 + M)$. ^{c} See text. ^{d} In this case p decreases with flow rate.

Figure 1. Period-2 oscillations for $j_0 = 4.824 \times 10^{-3}$ min^{-1}: time series (a), 2D view (b), and power spectrum (c).

peroxide concentration in the input flow was $[H_2O_2]_{in} = 0.155$ mol/dm^3. The results are summarized in Table 2.

At low j_0 values, only stable steady states were observed. A supercritical Hopf bifurcation occurs between $j_0 = 0.299 \times 10^{-3}$ and 0.300×10^{-3} min^{-1} as the stable steady-state becomes
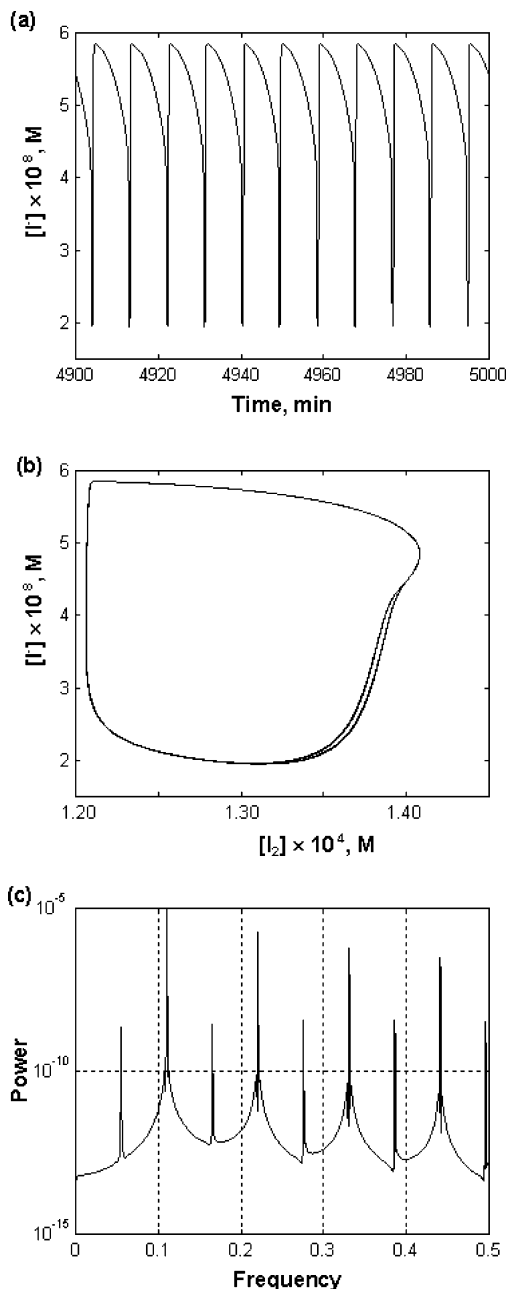
unstable and surrounded by a stable limit cycle. Afterward, the system exhibits simple oscillations with increasing amplitudes as the limit cycle grows and transforms acquiring a shape typical for relaxation oscillations. At $j_0 = 4.8237 \times 10^{-3}$ min^{-1} a period-doubling bifurcation occurs. This is practically impossible to notice in the time series (Figure 1a) but is evident looking at the projections of the trajectories from the 6D phase space onto a 2D subspace. Figure 1b shows that two successive oscillations are different. A Poincaré section for $[I^-] = 4 \times 10^{-8}$ mol/dm^3 gives exactly two intersection points at each side of the cycle. The power spectrum in Figure 1c shows a main peak at the frequency 0.110 min^{-1}, corresponding to one oscillation, a smaller peak at half this frequency, corresponding to the period-2 cycle, and their harmonics. When the flow rate is further increased, a period-doubling cascade was observed. As in the previous case, these bifurcations are not easily observable in the time series (Figure 2a). Very small differences with simple
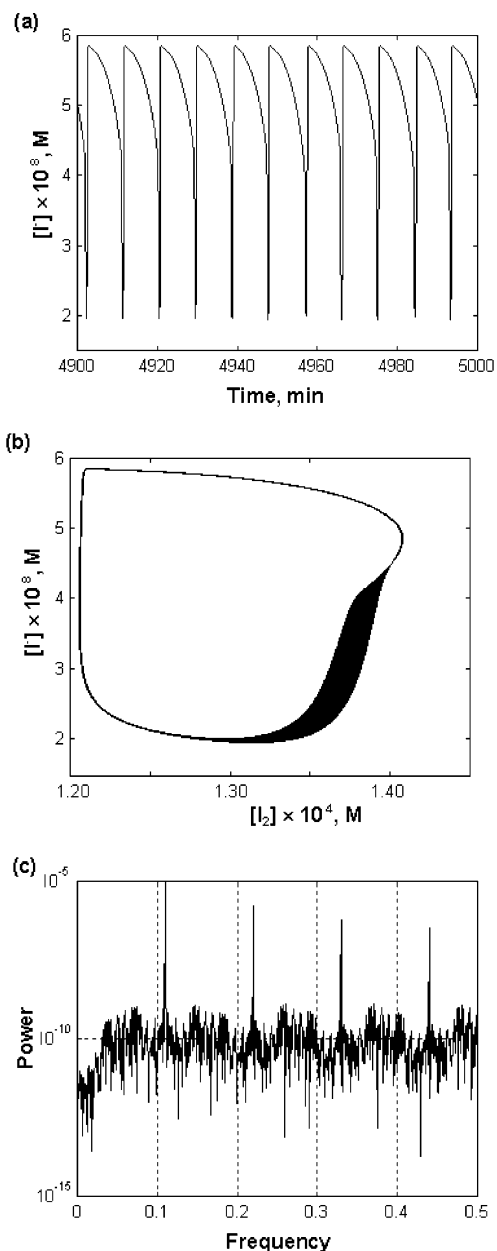
Figure 2. Chaos for $j_0 = 4.825 \times 10^{-3}$ min^{-1}: time series (a), 2D view (b), and power spectrum (c).

Figure 3. Time series of mixed-mode oscillations for $j_0 = 4.830 \times 10^{-3}$ (a), 4.863×10^{-3} (b), and 4.990×10^{-3} min^{-1} (c).

oscillations appear in some time series but the trajectories remain so close to that found at lower j_0 values that only a careful examination of the numerical results reveals the bifurcations. The j_0 values where the period 2^n appear, with $n = 1-5$, give successive Feigenbaum scaling numbers[38] equal to 5.6, 5.3, and 4.7 near to the asymptotical value 4.669. The calculated accumulation point[38] is at $j_0 = 4.82479 \times 10^{-3}$ min^{-1} and, actually, chaos is numerically observed from this value. The well-separated curves in Figure 1b are replaced by a continuous strip in Figure 2b. This indication of chaos is confirmed by the power spectrum given in Figure 2c. Peaks at the frequency 0.110 min^{-1} and at its higher harmonics emerge from a noisy background. The inverse of this frequency is the mean time to complete a turn of the attractor shown in Figure 2b and come back at *approximately* the same point (a chaotic trajectory never comes back at exactly the same point). The background is noisy because the actual trajectory wanders chaotically around a mean curve reminiscent of the former limit cycle. Argould et al.[37] have observed a similar behavior in the Belousov−Zhabotinsky
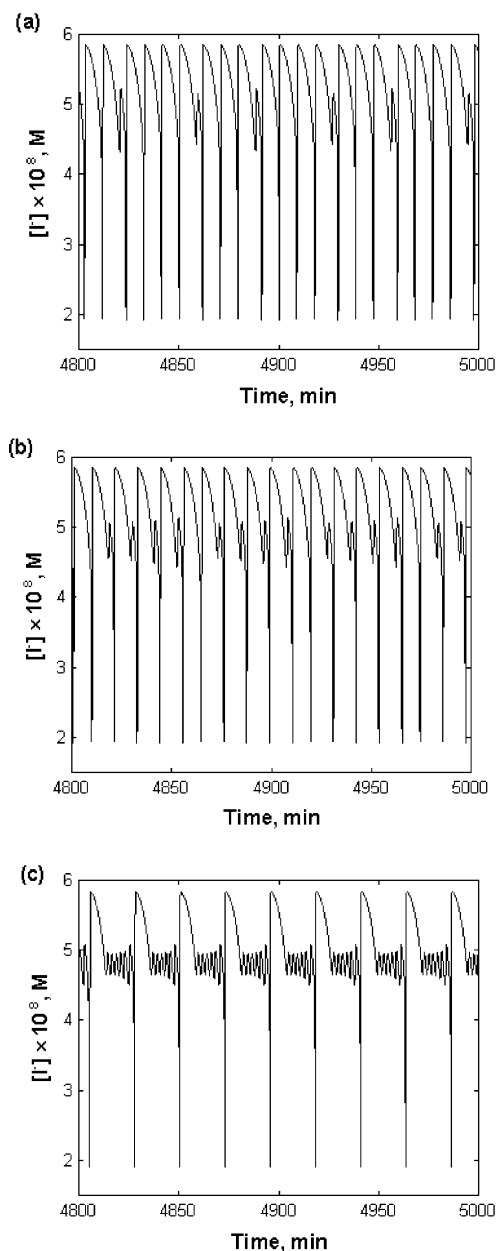
reaction and called it "microscopic chaos", because the chaotic attractor remains located in a tiny region of the phase space.

The domain of j_0 values giving chaos is very narrow and at $j_0 = 4.825\,93 \times 10^{-3}$ min^{-1} the oscillations are again periodic. The example given in Figure 3a shows that these periodic oscillations differ from the ones obtained at lower j_0 values, because they are now separated by small oscillations. The large amplitude oscillations are of the relaxation type whereas the small ones resemble modulated quasi-sinusoidal waves. The amplitudes of the large oscillations in a pattern are close to one another whereas the amplitudes of the small ones are different and depend on their number between two large oscillations. We describe the pattern of these mixed-mode oscillations using the notation of Maselko and Swinney.[39] The symbol l^s in a pattern denotes that a sequence of l consecutive large amplitude oscillations is followed by s consecutive small ones. For example, one period in Figure 3a is represented by [$4^1\ 3^1$] and in Figure 3b by [$2^1\ (1^1)_3$]. The notation $(1^1)_3$ means that we have three successive sequences 1^1, which must be different in one pattern
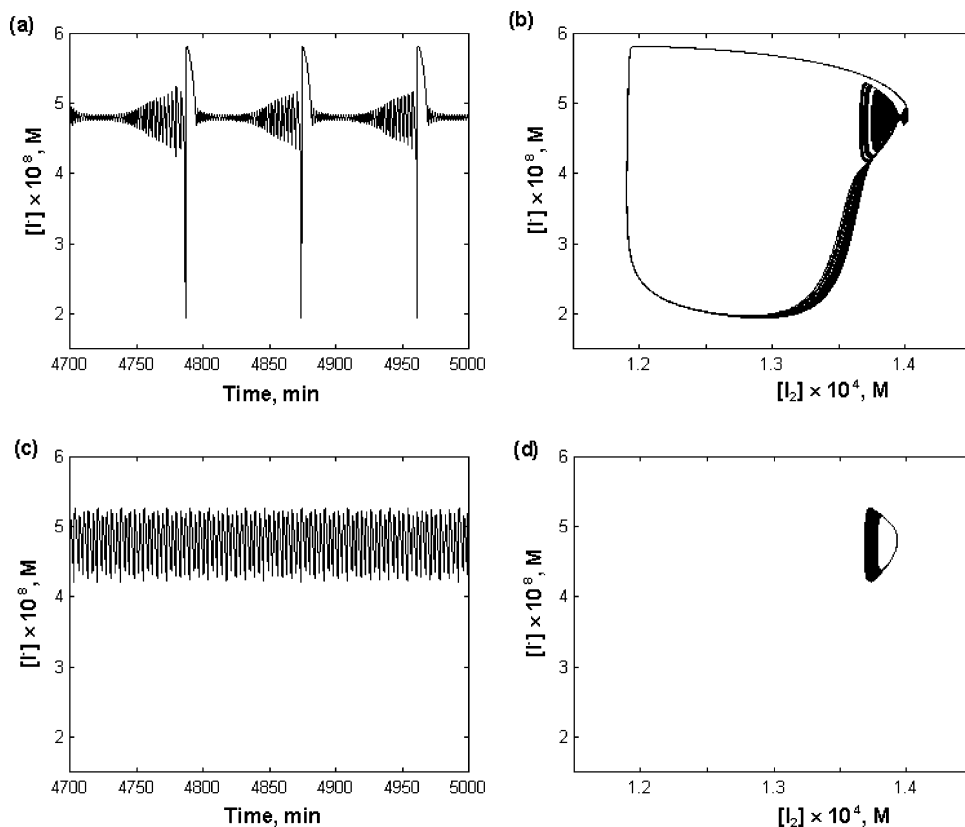
Catalytic H$_2$O$_2$ Decomposition

J. Phys. Chem. A, Vol. 110, No. 34, 2006 **10365**

Figure 4. Bifurcation from a chaotic mixture of large and small amplitude oscillations at $j_0 = 5.0812 \times 10^{-3}$ min^{-1} (a, b) to a small chaotic attractor at $j_0 = 5.0816 \times 10^{-3}$ min^{-1} (c, d).

because an oscillation identical to a former one indicates that the trajectory closes ending a period. The number of consecutive large and small oscillations should not be confused with the total number of large (L) and small (S) oscillations in a period. For example, the pattern $[2^1 (1^1)_3]$ gives $L = 5$ and $S = 4$. Values of the mean number of small oscillations in a period, $M = S/L$, are included in Table 2. M increases with j_0, as discussed in details hereafter, until a new bifurcation occurs at about $j_0 = 5.0811 \times 10^{-3}$ min^{-1}. The periodic pattern $[1^{35}]$ at $j_0 = 5.0810 \times 10^{-3}$ min^{-1} is replaced by a chaotic attractor shown in Figure 4a,b for $j_0 = 5.0812 \times 10^{-3}$ min^{-1}. When j_0 increases, the amplitude of the large oscillations does not change but the mean number of small amplitude oscillations between two large ones increases. It fluctuates from 35 to 40 at $j_0 = 5.0812 \times 10^{-3}$ min^{-1} and from 35 to about 130 at $j_0 = 5.0815 \times 10^{-3}$ min^{-1}, without any regularity. Near $j_0 = 5.0816 \times 10^{-3}$ min^{-1} a new phenomenon occurs. The dynamic remains chaotic but the large amplitude oscillations disappear, leaving a small attractor shown in Figure 4c,d. This sudden change of the size of the attractor suggests that we have a phenomenon known in the literature as a crisis.[38] The subsequent evolution is the reverse of a classical one: periodic oscillations in a sequence of period-halving, a small limit cycle, a reverse Hopf bifurcation near $j_0 = 5.120 \times 10^{-3}$ min^{-1} and a stable steady state.

We discuss now the evolution of the mixed-mode patterns when j_0 increases. At the beginning, the patterns show several large amplitude oscillations separated by only one small amplitude oscillation $[l^1]$. The number of large oscillations decreases until the state $[1^1]$ is reached. At higher j_0 values, the patterns show only one large oscillation and several small ones $[1^s]$ (Figure 3c). The region of mixed-mode oscillations ends at the bifurcation discussed before at about $j_0 = 5.0811 \times 10^{-3}$ min^{-1}. Between two simple patterns $[l^1]$ and $[(l-1)^1]$ or $[1^s]$ and $[1^{s+1}]$, complex patterns formed by their concatenation $[(l^1)((l-1)^1)_m]$

or $[(1^s)_n(1^{s+1})_m]$ are obtained. In the periodic dynamic states we have never found concatenation of patterns $[l^1]$ and $[(l-x)^1]$ or $[1^s]$ and $[1^{s+x}]$, where x is an integer larger than 1. Before the states $[l^1]$ and $[1^s]$, sequences of peak-adding $[(l+1)^1(l^1)_n]$ and $[1^{s-1}(1^s)_n]$ occur, where n seems to go to infinity, whereas after the $[l^1]$ and $[1^s]$ dynamic states, sequences corresponding to period-doublings, $[(l^1)_{2^p}]$ and $[(1^s)_{2^p}]$, where $p = 1, 2, 3, ...,$ leading to chaotic windows are observed (Table 2). [Scott (ref 40, p 88) has pointed out that the term peak-adding is more appropriate than period-adding because "...the sequence sees an increase in the number of individual excursions that go to form a total repeating unit..."]. We have carefully studied this period-doubling route to chaos by making 2D projections and Poincaré sections and by calculating the corresponding power spectra. The case $[1^1]$ is illustrated in Figure 5. The difference between the power spectra in Figure 5d,f for $j_0 = 4.8831 \times 10^{-3}$ and 4.8835×10^{-3} min^{-1} is striking. In the first case, the pattern is $[(1^1)_4]$ and we observe only a main peak at $f = 0.0865$ min^{-1}, corresponding to one oscillation, a peak at $f/4$, corresponding to a period, and their harmonics. In the second case, we still see the frequency 0.0865 min^{-1}, because the trajectory remains approximately in the same region of the phase space (we have microscopic chaos), but the sharp peaks are replaced by noise. The number of small amplitude oscillations between two large ones is distributed randomly between 1 and 2 with sometimes two consecutive large amplitude oscillations. No hysteresis was found at the borders of the chaotic windows. In the region of the mixed-mode oscillations, beside the chaotic windows that appear through period-doubling sequences, there are also chaotic windows consisting of chaotic mixtures of mixed-mode patterns.

In summary, by increasing j_0, we observe different kinds of simple, complex and chaotic oscillations between two stable steady states. On both borders between stable and unstable
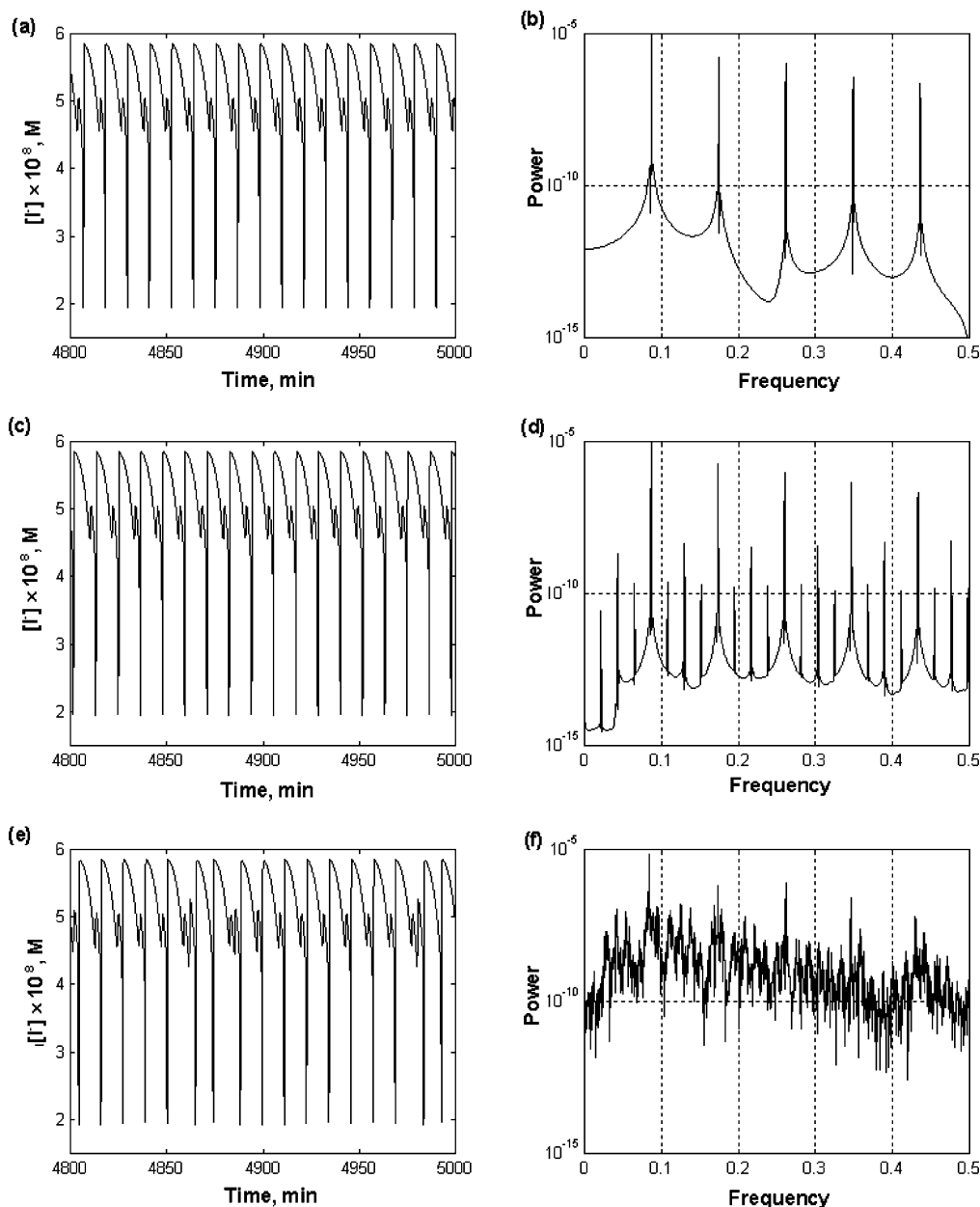
Figure 5. Time series and power spectra showing a period-doubling sequence leading to chaos: $j_0 = 4.8800 \times 10^{-3}$ min^{-1}, pattern [1^1] (a, b); $j_0 = 4.8831 \times 10^{-3}$ min^{-1}, pattern [$(1^1)_4$] (c, d); $j_0 = 4.8835 \times 10^{-3}$ min^{-1}, chaos (e, f).

steady states, there is a supercritical Hopf bifurcation. The general scheme of the evolution is the following.

Hopf → period-doubling cascade → chaos→
          mixed-mode oscillations → chaos →
                    period-halving cascade → Hopf

However, period-doubling cascades and chaotic windows inside the region of mixed-mode oscillations break this simple scenario. Moreover, there are differences between the two borders of this region. At low flow rates, the simple small amplitude oscillations emerging from the Hopf bifurcation quickly increase to large amplitude relaxation ones and the small amplitude oscillations appear inside the chaotic region. At high flow rates, the large amplitude oscillations disappear inside the chaotic region andonly small and quasi-sinusoidal oscillations between this region and the reverse Hopf bifurcation were found. Similar bifurcations were observed with different [H_2O_2]$_{in}$ but occur at lower j_0 values when [H_2O_2]$_{in}$ is higher.

Firing Numbers

The ratio $F = S/(L + S)$, called the firing number,[39,41−43] is related to the mean number of small oscillations given in Table 2 by $F = M/(1 + M)$. Figure 6 shows the increase of F with j_0 and plateaus where F does not change over a range of j_0 values. Our results agree with the expected behavior of F, similar to the behavior of winding numbers: the plateaus are larger when the values of the denominator $L + S$ are smaller. Hence, the largest plateau is obtained for $F = 1/2$, the next ones for $F = 1/3$ and $2/3$ and so on. As the firing number can be equal to any rational fraction, there is an infinite number of such plateaus and they form a so-called devil's staircase.[38,39,41−43] In the investigated system, chaotic windows at the end of the stairs interrupt the devil's staircase. These windows are preceded by period-doubling sequences and cover the beginning of the subsequent peak-adding evolutions. Also, both ends of the staircase ($F = 0$ and $F = 1$) are missing. The smallest observed value is $F = 1/7$ for the pattern [6^1] when $j_0 = 4.825\ 93 \times 10^{-3}$ min^{-1}.

Catalytic H$_2$O$_2$ Decomposition

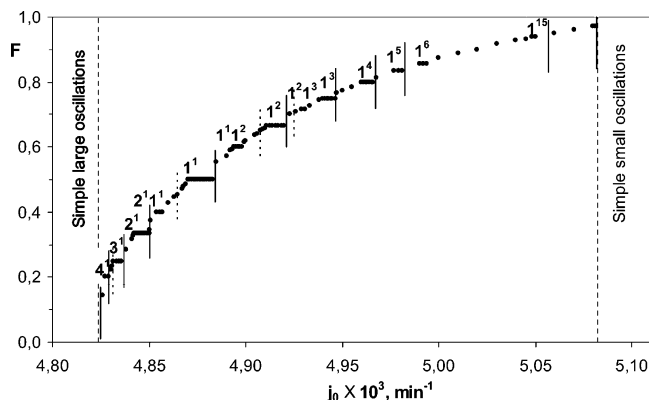*J. Phys. Chem. A, Vol. 110, No. 34, 2006* **10367**

Figure 6. Devil's staircase in the region of complex oscillations (●), chaos after a period-doubling sequence (|) and chaos breaking periodic mixed-mode sequences (⋮).

Below this value, between $j_0 = 4.825\,80 \times 10^{-3}$ and $4.825\,92 \times 10^{-3}$ min^{-1}, the motion is chaotic as in Figure 2 but with added small amplitude oscillations announcing the mixed-mode regime. The largest observed value is $F = {}^{35}/_{36}$ for the pattern $[1^{35}]$ when $j_0 = 5.0810 \times 10^{-3}$ min^{-1}. Above this value, between $j_0 = 5.0812 \times 10^{-3}$ and 5.0816×10^{-3} min^{-1}, the motion is chaotic.

Denoting by $j_{0,M}$ the smallest value of j_0 on a plateau, j_{min} the value of j_0 such that $F = 0$, and j_{max} the value of j_0 such that $F = 1$, we have found that F and $j_{0,M}$ are related by the following simple relation

$$M = \frac{F}{1-F} = k_M \frac{j_{0,M} - j_{min}}{j_{max} - j_{0,M}}$$

The values $j_{min} = 4.8084 \times 10^{-3}$ min^{-1} and $j_{max} = 5.1089 \times 10^{-3}$ min^{-1} are determined by extrapolation of j_0 to $F = 0$ and $F = 1$, respectively. k_M is an empirical constant given in Table 2. The constancy of k_M is noteworthy and suggests some as yet unrevealed theoretical explanation.

Discussion and Conclusions

The examined model for the BL reaction simulates a number of periodic and aperiodic dynamic states under CSTR conditions: stable steady states, supercritical Hopf bifurcation, simple oscillations changing their form from small amplitude quasi-sinusoidal oscillations to large amplitude relaxation ones, successive period-doublings ending with chaos, peak-adding with dynamic states changing from several large amplitude oscillations with one small amplitude oscillation to states with single large amplitude oscillations separated by small amplitude modulated waves, period-halving before small amplitude sinusoidal oscillations and a reverse Hopf bifurcation point at the end of the domain where the steady state is unstable. Within this domain, transition from a former to the following simple mixed-mode state occurs through period-doublings, leading to a chaotic window in which the subsequent dynamic state emerges mixed with the preceding one. Thus we have the period-doubling route to chaos by increasing the flow rate and the peak-adding route to the same state by increasing the residence time. For example, in the region with several large and only one small amplitude oscillations the following sequence of dynamic states was observed

$$[l^1] \rightarrow [(l^1)_2] \rightarrow [(l^1)_4] \rightarrow [(l^1)_8] \rightarrow ... \rightarrow \text{chaos} \rightarrow ... \rightarrow$$
$$[(l^1)_3(l-1)^1] \rightarrow [(l^1)_2(l-1)^1] \rightarrow [l^1(l-1)^1] \rightarrow$$
$$[l^1((l-1)^1)_2] \rightarrow [l^1((l-1)^1)_3] \rightarrow ... \rightarrow [(l-1)^1]$$

or, in the region with one large amplitude and several small amplitude oscillations,

$$[1^s] \rightarrow [(1^s)_2] \rightarrow [(1^s)_4] \rightarrow [(1^s)_8] \rightarrow ... \rightarrow \text{chaos} \rightarrow ... \rightarrow$$
$$[(1^s)_3\, 1^{s+1}] \rightarrow [(1^s)_2\, 1^{s+1}] \rightarrow [1^s\, 1^{s+1}] \rightarrow [1^s\, (1^{s+1})_2] \rightarrow$$
$$[1^s\, (1^{s+1})_3] \rightarrow ... \rightarrow [1^{s+1}]$$

Moreover, in very narrow regions of flow rates, chaotic mixtures of mixed-mode patterns have been found (denoted by ⋮ in Figure 6). This complex evolution of the system is more obvious in dynamic states with small s and l values, that is, for firing numbers about 0.5. For firing numbers close to 0 and 1, the different dynamic states are practically merged to one another and very difficult for complete numerical illustration.

The number of chaotic windows depends on the number of simple $[l^s]$ dynamic states. Although this number would go to infinity in the complete region of mixed-mode oscillations, the number of chaotic windows is finite because the beginning and the end of the region of mixed-mode oscillations are covered by chaotic regions (in the simulations we obtained only states from $[6^1]$ to $[1^{35}]$). All these states cannot be found numerically because some of them would be realized in very narrow regions of flow rates that are affected by the precision of the numerical calculations.

The mixed-mode region ends at high flow rates corresponding to chaotic states characterized by a mixture of one large oscillation followed by trains of small amplitude oscillations—we observed s values up to 130 in this chaotic region. Starting from the reverse Hopf bifurcation point and going in the opposite direction, i.e., decreasing the flow rate, we first encounter simple small amplitude sinusoidal oscillations and then a period-doubling route to chaos. When the flow rate is decreased further, mixed-mode oscillations emerge through a dynamic state with one large and numerous small amplitude oscillations. This progression is a mirrored image of the previously explained evolution for increasing the specific flow rate starting with very low flows.

The discussed dynamic states together with numerous other phenomena found in real experiments conducted under batch and CSTR conditions are simulated by the proposed model for the BL reaction with the rate constants listed in Table 1.[24−27,30,31,33−35] Under batch conditions the correlation between modeled and experimentally measured concentrations, duration of the oscillatory cascade, length of the smooth evolution preceding the oscillations, period of the oscillations, reinstatement of the oscillatory state after dilution and others were examined. In these cases even quantitative agreement is achieved. In the CSTR, only qualitative relations between experimentally observed and modeled phenomena, Hopf bifurcations, simple relaxation oscillations, mixed-mode oscillations and chaotic windows, were found. It is particularly important that these dynamic states can be simulated by the proposed model because it does not include any direct autocatalytic or auto-inhibition step in the form A + xB → ($x \pm 1$)B that would induce nonlinearity. Here, the main feedback comes from the competition between reactions R5 and R6. Hydrogen peroxide acts as a reducing agent in reaction R5 with a rate proportional to [HIO] and as an oxidizing agent in reaction R6 with a rate proportional

to [I$_2$O], that is, with reaction R-3, proportional to the square of [HIO]. An increase of [HIO] favors the oxidation (R6) with respect to the reduction (R5), causing in this way a further increase of [HIO].[44] Moreover, the analyzed model is based exclusively on liquid-phase reactions and does not account for the escape of volatile and gaseous species from the liquid phase that can be an additional source of nonlinearity.

The major discrepancy between the model predictions and the real experiments under CSTR conditions[24,25] is reflected in the form of mixed-mode oscillations. Namely, in numerical simulations small amplitude oscillations in the mixed-mode region emerge at the end of the reduction pathway whereas they are observed experimentally at the end of the oxidation pathway. This suggests that contributions of the pathways (R) and (O) that exist in the model should be rearranged by adjusting the proposed set of rate constants and, eventually, the model would be corrected. For this purpose, besides the present knowledge, more information about the individual reactions between the iodine compounds[45,46] and about the subsets (R) and (O)[47] is required.

The behaviors observed by analyzing the model for the BL reaction characterized by peak-adding evolution from [l^1] to [1^s] and mixed-mode regions with patterns formed by concatenations between successive simple patterns are globally similar but different from that obtained experimentally in the Belousov–Zhabotinsky reaction[37,39,40,48] or numerically in this and other systems.[41,48–52] Chaotic windows appearing through period-doubling and disappearing through peak-adding sequences were not observed in these systems. Hence, the examinations of the model of the BL reaction together with new obtained results are of general importance for modeling and predicting the behavior of other oscillatory processes.

References and Notes

(1) Bray, W. C. *J. Am. Chem. Soc.* **1921**, *43*, 1262.
(2) Bray, W. C.; Liebhafsky, H. A. *J. Am. Chem. Soc.* **1931**, *53*, 38.
(3) Matsuzaki, I.; Woodson, J. H.; Liebhafsky, H. A. *Bull. Chem. Soc. Jpn.* **1970**, *43*, 3317.
(4) Liebhafsky, H. A.; Wu, L. S. *J. Am. Chem. Soc.* **1974**, *96*, 7180.
(5) Sharma, K. R.; Noyes, R. M. *J. Am. Chem. Soc.* **1976**, *98*, 4345.
(6) Liebhafsky, H. A.; Furuichi, R.; Roe, G. M. *J. Am. Chem. Soc.* **1981**, *103*, 51.
(7) Odutola, J. A.; Bohlander, C. A.; Noyes, R. M. *J. Phys. Chem.* **1982**, *86*, 818.
(8) Furrow, S. D. In *Oscillations and Traveling Waves in Chemical Systems*; Field, R. J., Burger, M., Eds.; J. Wiley: New York, 1985; p 171.
(9) Anić, S.; Mitić, D.; Kolar-Anić, Lj. *J. Serb. Chem. Soc.* **1985**, *50*, 53.
(10) Anić, S.; Kolar-Anić, Lj. *Ber Bunsen-Ges. Phys. Chem.* **1986**, *90*, 1084.
(11) Schmitz, G. *J. Chim. Phys.* **1987**, *84*, 957.
(12) Anić, S.; Kolar-Anić, Lj. *J. Chem. Soc., Faraday Trans. 1* **1988**, *84*, 3413.
(13) Buchholtz, F. G.; Broecker, S. *J. Phys. Chem. A* **1988**, *102*, 1556.

(14) Anić, S.; Stanisavljev, D.; Krnajski Belovljev, G.; Kolar-Anić, Lj. *Ber Bunsen-Ges. Phys. Chem.* **1989**, *93*, 488.
(15) Schmitz, G. In *Spatial inhomogeneities and transient behaviour in chemical kinetics*; Gray, P., Nicolis, G., Baras, F., Borkmans, P., Scott, S. K., Eds.; Manchester University Press: Manchester, U.K., 1990; p 666.
(16) Ševčík, P.; Adamčíková, L. *Chem. Phys. Lett.* **1997**, *267*, 307.
(17) Anić, S.; Stanisavljev, D.; Čupić, Ž.; Radenković, M.; Vukojević, V.; Kolar-Anić, Lj. *Sci. Sintering* **1998**, *30*, 49.
(18) Stanisavljev, D.; Begović, N.; Žujović, Z.; Vučelić, D.; Bačić, G. *J. Phys. Chem. A* **1998**, *102*, 6883.
(19) Stanisavljev, D.; Begović, N.; Vukojević, V. *J. Phys. Chem. A* **1998**, *102*, 6887.
(20) Vîlcu, R.; Danciu, T.; Bala, D. *Discrete Dynam. Nature Soc.* **2000**, *4*, 55.
(21) Ševčík, P.; Kissimonová, K.; Adamčíková, L. *J. Phys. Chem. A* **2000**, *104*, 3958.
(22) Ćirić, J.; Anić, S.; Čupić, Ž.; Kolar-Anić, Lj. *Sci. Sintering* **2000**, *32*, 187.
(23) Stanisavljev, D. R.; Đorđević, A. R.; Likar-Smiljanić, V. D. *ChemPhysChem* **2004**, *5*, 140.
(24) Vukojević, V.; Anić, S.; Kolar-Anić, Lj. *J. Phys. Chem. A* **2000**, *104*, 10731.
(25) Kolar-Anić, Lj.; Vukojević, V.; Pejić, N.; Grozdić, T.; Anić, S. In *Experimental Chaos*; Boccaletti, S., Gluckman, B. J., Kurths, J., Pecora, L., Meucci, R., Yordanov, O., Eds; AIP Conference Proceedings, Vol. 742; American Institute of Physics: Melville, NY, 2004; p 3.
(26) Kolar-Anić, Lj.; Schmitz, G. *J. Chem. Soc., Faraday Trans.* **1992**, *88*, 2343.
(27) Kolar-Anić, Lj.; Mišljenović, Đ.; Anić, S.; Nicolis, G. *React. Kinet. Catal. Lett.* **1995**, *54*, 35.
(28) Kolar-Anić, Lj.; Grozdić, T.; Vukojević, V.; Schmitz, G.; Anić, S. In *Selforganization in nonequilibrium systems*; Anić, S., Čupić, Ž., Kolar-Anić, Lj., Eds.; Society of Physical Chemists of Serbia: Belgrade, 2004; p 115.
(29) Schmitz, G. *Phys. Chem. Chem. Phys.* **1999**, *1*, 4605.
(30) Kolar-Anić, Lj.; Mišljenović, Đ.; Stanisavljev, D.; Anić, S. *J. Phys. Chem.* **1990**, *94*, 8144.
(31) Radenković, M.; Schmitz, G.; Kolar-Anić, Lj. *J. Serb. Chem. Soc.* **1997**, *62*, 367.
(32) Kolar-Anić, Lj.; Čupić, Ž.; Anić S.; Schmitz, G. *J. Chem. Soc., Faraday Trans.* **1997**, *93*, 2147.
(33) Valent, I.; Adamčíková, L.; Ševčík, P. *J. Phys. Chem. A* **1998**, *102*, 7576.
(34) Kissimonová, K.; Valent, I.; Adamčíková, L.; Ševčík, P. *Chem. Phys. Lett.* **2001**, *341*, 345.
(35) Vukojević, V.; Anić, S.; Kolar-Anić, Lj. *Phys. Chem. Chem. Phys.* **2002**, *4*, 1276.
(36) Clarke, B. L. *Adv. Chem. Phys.* **1980**, *43*, 1.
(37) Argoul, F.; Arneodo, A.; Richetti, P.; Roux, J. C. *J. Chem. Phys.* **1987**, *86*, 3325.
(38) Hilborn, R. C. *Chaos and Nonlinear Dynamics*, 2nd ed.; Oxford University Press: Oxford, U.K., 2000.
(39) Maselko, J.; Swinney, H. L. *J. Chem. Phys.* **1986**, *85*, 6430.
(40) Scott, S. K. *Oscillations, Waves and Chaos in Chemical Kinetics*; Oxford University Press: Oxford, U.K., 2004.
(41) Kim, K. R.; Shin, K. J.; Lee, D. J. *J. Chem. Phys.* **2004**, *121*, 2664.
(42) Larter, R.; Bush, C. L.; Lonis, T. R.; Aguda, B. D. *J. Chem. Phys.* **1987**, *87*, 5765.
(43) Scott, S. K. *Chemical Chaos*; Clarendon Press: Oxford, U.K., 1997.
(44) Schmitz, G. *J. Chim. Phys.* **1991**, *88*, 15.
(45) Schmitz, G. *Int. J. Chem. Kinet.* **2004**, *36*, 480.
(46) Begović, N.; Marković, Z.; Anić, S.; Kolar-Anić, Lj. *J. Phys. Chem. A* **2004**, *108* 651.
(47) Schmitz, G. *Phys. Chem. Chem. Phys.* **2001**, *3*, 4741.
(48) Kalishin, E. Yu.; Goncharenko, M. M.; Khavrus, V. A.; Strizhak, P. E. *Kinet. Catal.* **2002**, *43*, 233.
(49) Richetti, P.; Roux, J. C.; Argoul, F.; Arneodo, A. *J. Chem. Phys.* **1987**, *86*, 3339.
(50) Barkley, D. *J. Chem. Phys.* **1988**, *89*, 5547.
(51) Kawczynski, A. L.; Khavrus, V. O.; Strizhak, P. E. *Chaos* **2000**, *10*, 299.
(52) Khavrus, V. O.; Strizhak, P. E.; Kawczynski, A. L. *Chaos* **2003**, *13*, 112.